A New Docking Domain Type in the Peptide-Antimicrobial-Xenorhabdus Peptide Producing nonribosomal Peptide Synthetase from *Xenorhabdus bovienii*

Jonas Watzel[1], Carolin Hacker[2], Elke Duchardt-Ferner[2], Helge B. Bode[1,3,4], Jens Wöhnert[2], Goethe University, Frankfurt/ Germany

1   Molecular Biotechnology, Institute of Molecular Biosciences, Goethe University Frankfurt, 60438, Frankfurt am Main, Germany.

2   Institute of Molecular Biosciences and Center for Biomolecular Magnetic Resonance (BMRZ), Goethe University Frankfurt, 60438, Frankfurt am Main, Germany.

3   Buchmann Institute for Molecular Life Sciences (BMLS), Goethe University Frankfurt, 60438, Frankfurt am Main, Germany.

4   Senckenberg Gesellschaft für Naturforschung, 60325, Frankfurt am Main, Germany

TABLE OF CONTENTS

SUPPORTING TABLES

Table S1. Strains used in this work.

Strain	Genotype / NRPS	Reference
E. coli BL21-Gold(DE3)	*E. coli* B F⁻ *ompT hsdS*(r$_B$⁻ m$_B$⁻) *dcm*⁺ Tet^r *gal* λ(DE3) *endA* Hte / -	(*1*)
Xenorhabdus bovienii SS-2004	wild type / *paxS (2)*	(*3*)

Table S2. Plasmids used in this work.

Plasmids	Description	Reference
pET11a-modified	modified from pET11a, the operon under the control of T7 promoter was modified by introduction of N-terminal His_6-smt3 tag, amp^R	(*4*)
pJW30	vector, the PaxB ^{C}DD was fused C-terminally to *smt3* into pET11a-modified, under control of T7 promoter, amp^R	this study
pJW31	vector, the PaxC ^{N}DD was fused C-terminally to *smt3* into pET11a-modified, under control of T7 promoter, amp^R	this study
pJW35	vector, the PaxC ^{N}DD-$(GS)_{12.5}$-PaxB ^{C}DD was fused C-terminally to smt3 into pET11a-modified, under control of T7 promoter, ampR	this study

Table S3. Oligonucleotides used in this work.

| Plasmids	Oligo-nucleotide	Sequence (5′→3′; overlapping ends)	Targeting DNA fragment	Template
pJW30 (PaxB ^{C}DD)	pET11a_FW	TAAGGATCCGGCTGCTAAC	pET11a-modified vector backbone	pet11a-modified
	pET11a_Smt3_RV	ACCACCAATCTGTTCACGA		pet11a-modified
	jw0017_FW	<u>CATCGTGAACAGATTGGTGGT</u>TATCAAATTGAAACTTTTTTCGC	PaxB ^{C}DD insert	*Xenorhabdus bovienii* SS-2004
	ck0045_RV	<u>TTTGTTAGCAGCCGGATCCTT</u>ATTGTTGATCTCCATTTAACATGG		*Xenorhabdus bovienii* SS-2004
pJW31 (PaxC ^{N}DD)	pET11a_FW	TAAGGATCCGGCTGCTAAC	pET11a-modified vector backbone	pet11a-modified
	pET11a_Smt3_RV	ACCACCAATCTGTTCACGA		pet11a-modified
	ck0042_FW	<u>CATCGTGAACAGATTGGTGGT</u>ATGAACATAAATGAACAAACTTTGG	PaxC ^{N}DD insert	*Xenorhabdus bovienii* SS-2004
	ck0016_RV	<u>TTTGTTAGCAGCCGGATCCTT</u>AATATTTTTCAGTACTCAGGCTGTTC		*Xenorhabdus bovienii* SS-2004
pJW35 (PaxC ^{N}DD-(GS)$_{12.5}$-PaxB ^{C}DD)	pET11a_FW	TAAGGATCCGGCTGCTAAC	pET11a-modified vector backbone	pet11a-modified
	pET11a_Smt3_RV	ACCACCAATCTGTTCACGA		pet11a-modified
	ck0042_FW	<u>CATCGTGAACAGATTGGTGGT</u>ATGAACATAAATGAACAAACTTTGG	PaxC ^{N}DD-(GS)$_{7.5}$ insert#1	*Xenorhabdus bovienii* SS-2004
	jw0022_RV	<u>ACCTGAACCACTACCCGAACCCGATCCGGAACCTGAACCACTACC</u>ATATTTTTCAGTACTCAGGCTGTTC		*Xenorhabdus bovienii* SS-2004
	jw0023_FW	<u>GGTAGTGGTTCAGGTTCCGGATCGGGTTCGGGTAGTGGTTCAGGT</u>TATCAAATTGAAACTTTTTTCGCC	(GS)$_{7.5}$-PaxB ^{C}DD insert#2	*Xenorhabdus bovienii* SS-2004
	ck0045_RV	<u>TTTGTTAGCAGCCGGATCCTT</u>ATTGTTGATCTCCATTTAACATGG		*Xenorhabdus bovienii* SS-2004

Table S4. Structural statistics for the NMR solution structures of PaxC [N]DD-(GS)$_{12.5}$-PaxB [C]DD. For the calculation PSVS 1.5 (*5*) was used.

	PaxC [N]DD-(GS)$_{12.5}$-PaxB [C]DD.
Conformationally-restricting experimental constraints[a]	
Total NOE distance restraints	1685
intraresidue |i = j|	420
sequential |i - j| = 1	517
medium-range 1 <|i - j| < 5	568
long-range |i - j| ≥ 5	180
NOE constraints per restrained residue[b]	25.5
Dihedral angle restraints (TALOS-N)	94
Total number of restricting constraints[b]	1779
Total number of restricting constraints per restrained residue[b]	27.0
Total number of long-range constraints per restrained residue[b]	2.7
Residual constraint violations[a,c]	
Average number of distance violations per structure	
0.1-0.2 Å	4.9
0.2-0.5 Å	0
>0.5 Å	0
Average number of dihedral angle violations per structure	
1-10	13.15
>10	0
Model quality (ordered residues)	
RMSD backbone atoms (Å)	0.4
RMSD heavy atoms (Å)	0.7
RMSD bond lengths (Å)	0.010
RMSD bond angles (°)	2.2
CYANA target function	2.24±0.35
Ramachandran Plot Statistics from Richardson's lab	
Most favored regions	90.5 %
Allowed regions	8.9 %
Disallowed regions	0.6 %
Global quality scores (raw/Z score)	
Verify3D	0.29/-2.73
Prosall	0.74/0.37
PROCHECK (φ-ψ)	-0.32/-0.94
PROCHECK (all)	-0.63/-3.73
MolProity clash score	7.36/0.26
Model contents	
Ordered residue ranges (user defined)	4-31, 60-90
Total no. of residues	93
Biological Magnetic Resonance Bank (BMRB) accession number	34469
Protein Databank (PDB) ID code	6TRP

[a] analysed for residues 1 to 93, [b] there are 66 residues with conformationally restricting constraints, [c] average distance violations were calculated using the sum over r^{-6}

SUPPORTING FIGURES
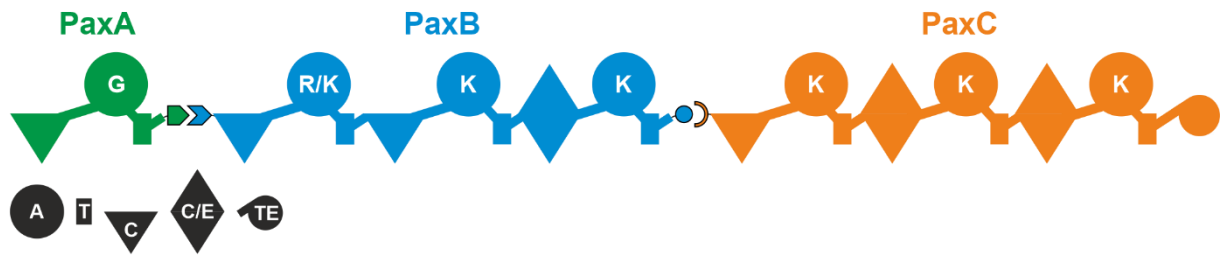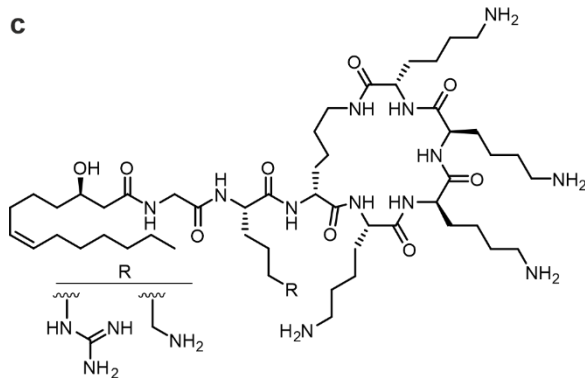

Figure S1. Peptide-antimicrobial-Xenorhabdus (PAX) producing NRPS. (a) Schematic illustration of the peptide-antimicrobial-Xenorhabdus (PAX) producing NRPS of *Xenorhabdus bovienii*. The analysed DD pair (boxed) was artificially linked by an 25 aa long glycine-serine (GS) linker. The NRPS consists of three polypeptides (PaxA/B/C) with an unidirectional interaction order. For domain assignment the following symbols are used: adenylation domain (A, large circle); thiolation domain (T, rectangle); condensation domain (C, triangle); dual condensation/epimerization domain (C/E, diamond); thioesterase domain (TE, C-terminal small circle). (b) Alignment of *Xenorhabdus bovienii* PaxA/B [C]DDs and PaxB/C [N]DDs. The amino acids are coloured in respect to their polarity. The Alignment was performed using the multiple alignment program MUSCLE (default parameters). (*6, 7*) (c) Structure of two major PAX peptides.
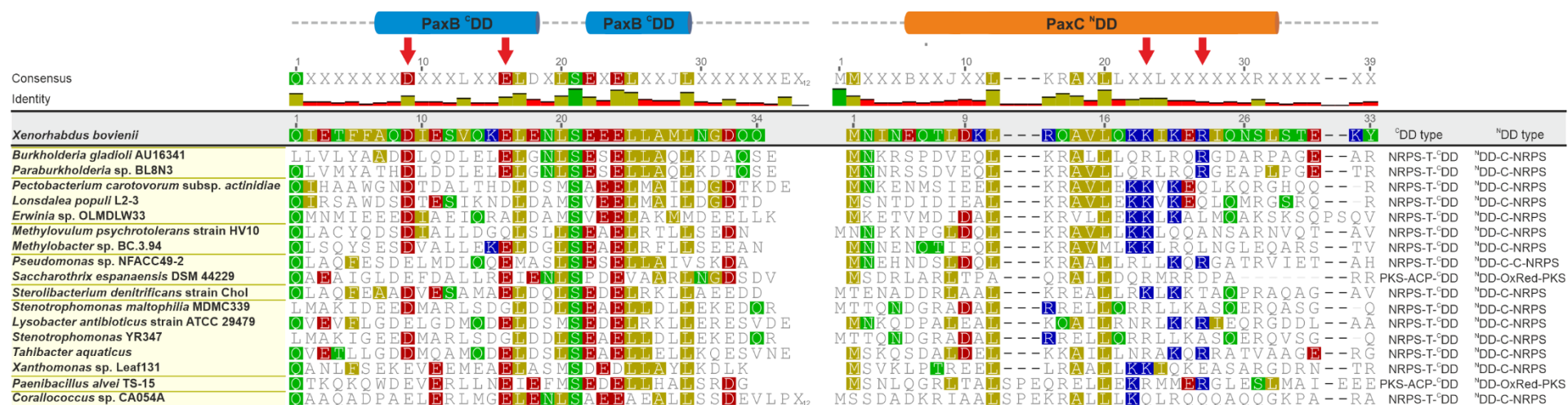
Figure S2. Alignment of selected NRPS/PKS ^CDDs and ^NDDs identified by BLASTp search using *Xenorhabdus bovienii* PaxB/C ^CDD/^NDDs with parts of the attached T or C domains as query sequences. Secondary structural elements are depicted above and arrows indicating salt bridge forming residues. Both annotations refer to the solved docking domain complex structure. The bacteria in the alignment are grouped by their order including (from top to bottom): Burkholderiales, Enterobacteriales, Methylococcales, Pseudonocardiales, Rhodocyclales, Xanthomonadales, Bacillales and Myxococcales. This docking domain type is widespread in the field of PKS and NRPS systems, connecting most commonly thiolation (T) and condensation (C) domains [NRPSs] besides acyl carrier proteins (ACPs) and oxidoreductase (OxRed) domains [PKSs]. The consensus alignment is depicted above the alignment sequences with a 50% threshold implemented. Amino acid agreements are highlighted by comparison with the *Xenorhabdus bovienii* reference sequences. Alignments were performed using the multiple sequence alignment program MUSCLE (default parameters). (*6, 7*)
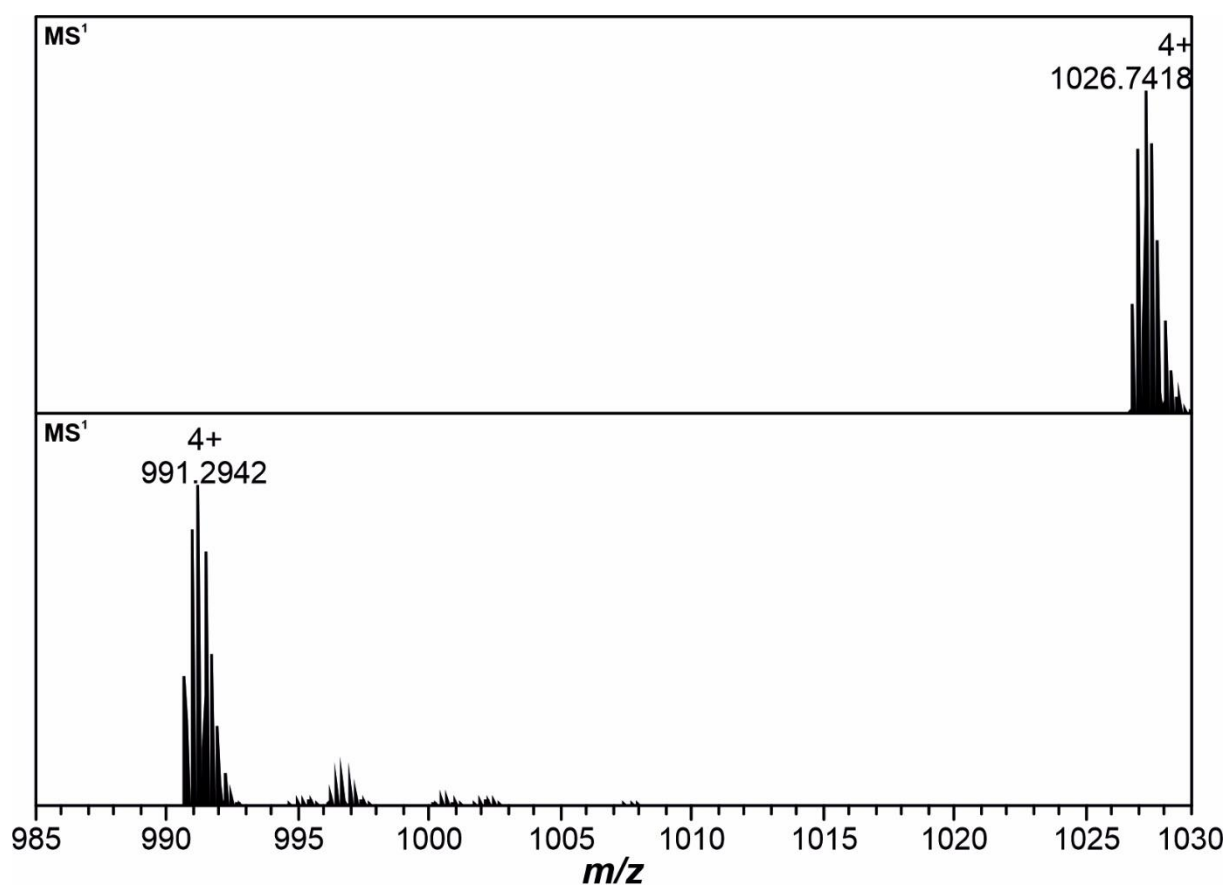
Figure S3. HR-HPLC-ESI-MS analysis of purified proteins. Displayed are the *m/z*-values of the average protein masses (PaxB ^{C}DD (top) and PaxC ^{N}DD (bottom)) of the 4+ charge states (MS^1). *m/z* 1026.7418 corresponds to PaxB ^{C}DD ($m/z_{theoretical}$ 1026.7440; Δppm 2.1) and *m/z* 991.2942 corresponds to PaxC ^{N}DD ($m/z_{theoretical}$ 991.2993; Δppm 5.1) in MS^1.
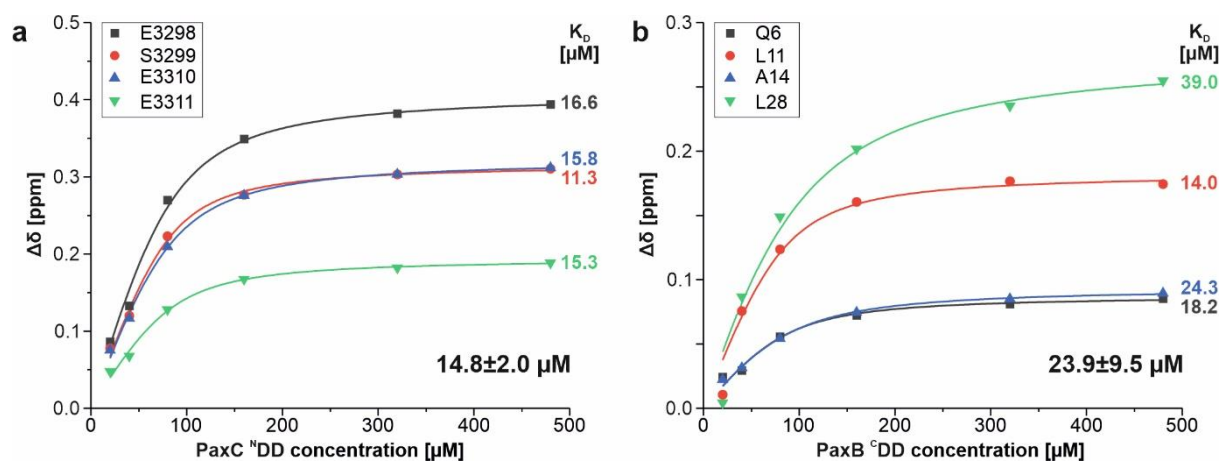
Figure S4. K_D determination based on NMR chemical shift data. The chemical shift changes caused by peptide binding are plotted against the respective peptide concentration for the (a) PaxB ^{C}DD and (b) PaxC ^{N}DD. The mean K_D values and standard deviations are given for residues (PaxB ^{C}DD: E3298, S3299, E3310, E3311; PaxC ^{N}DD: Q6, L11, A14, L28) which are all in the fast exchange regime.
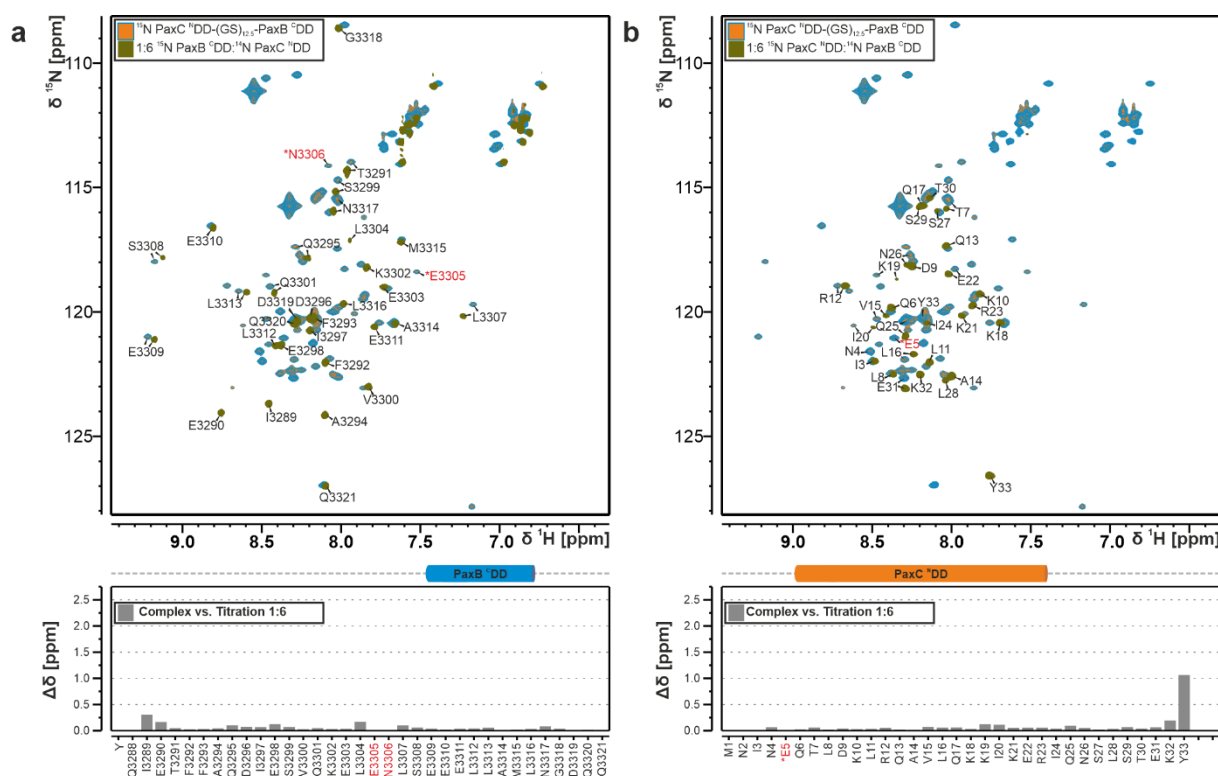
Figure S5. Chemical shift comparison of the unlinked and the GS-linked DD complex. Overlay of $^1H,^{15}N$-HSQC spectra (top) of (a) 80 µM ^{15}N-labeled PaxB ^CDD upon addition of a six-fold molar excess of unlabelled PaxC ^NDD and ^{15}N-labeled PaxC ^NDD-(GS)$_{12.5}$-PaxB ^CDD; bar chart of chemical shift differences between titration endpoint [1:6 molar ratio] and DD complex plotted against the residues of PaxB ^CDD (bottom). (b) 80 µM ^{15}N-labeled PaxC ^NDD upon addition of a six-fold molar excess of unlabelled PaxB ^CDD and ^{15}N-labeled PaxC ^NDD-(GS)$_{12.5}$-PaxB ^CDD; bar chart of chemical shift differences between titration endpoint [1:6 molar ratio] and DD complex plotted against the residues of PaxC ^NDD (bottom). For residues coloured red and marked with an asterisk (*) no peaks could be clearly identified at the titration endpoint due to peak overlap but these were easily identified in the GS-linked complex.
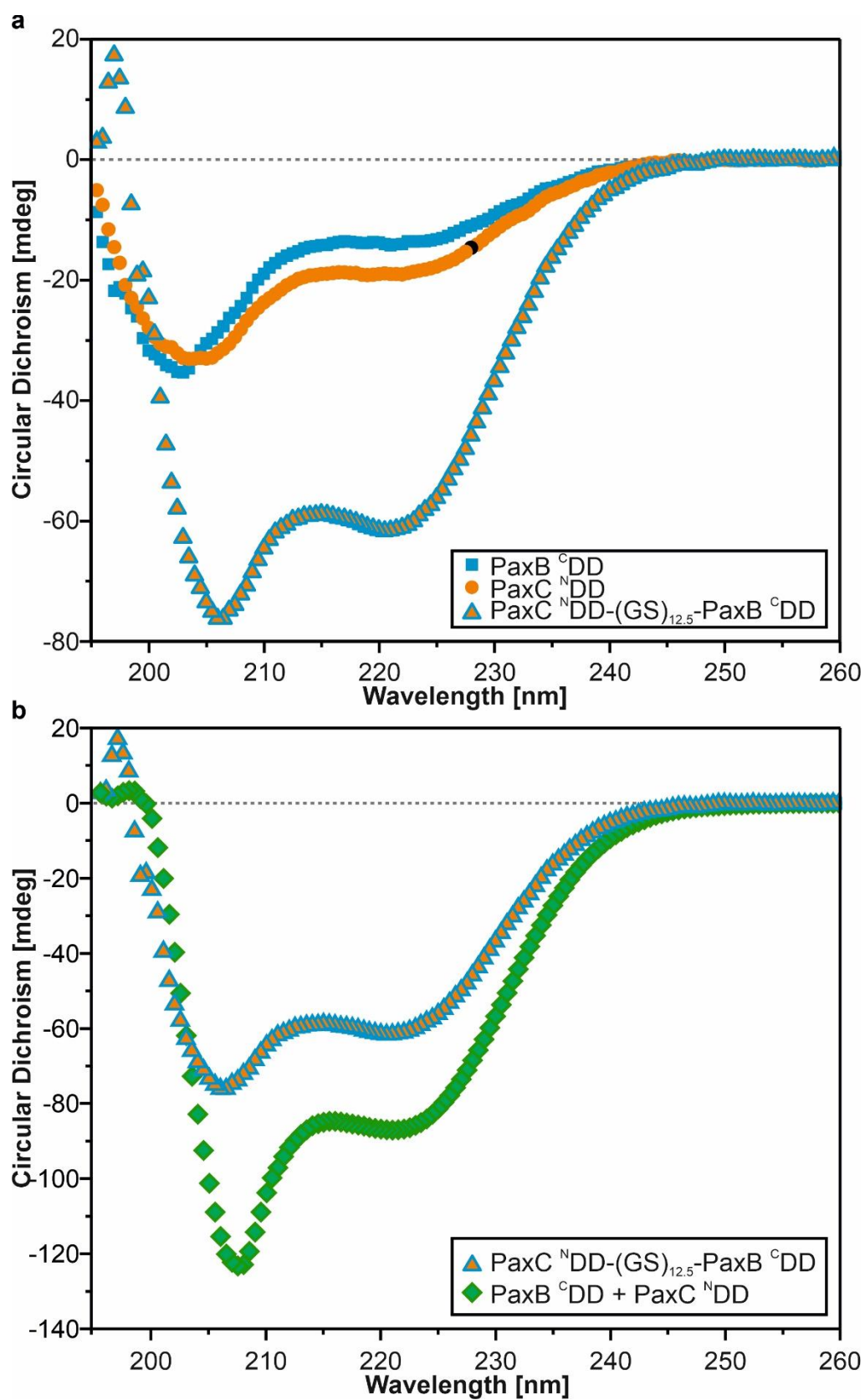
Figure S6. Overlay of circular dichroism spectra. (a) 50 µM PaxB/C $^{C/N}$DD and PaxC ^{N}DD-(GS)$_{12.5}$-PaxB ^{C}DD samples and (b) of 50 µM PaxC ^{N}DD-(GS)$_{12.5}$-PaxB ^{C}DD and unlinked PaxB ^{C}DD:PaxC ^{N}DD (120 µM of each DD) samples.
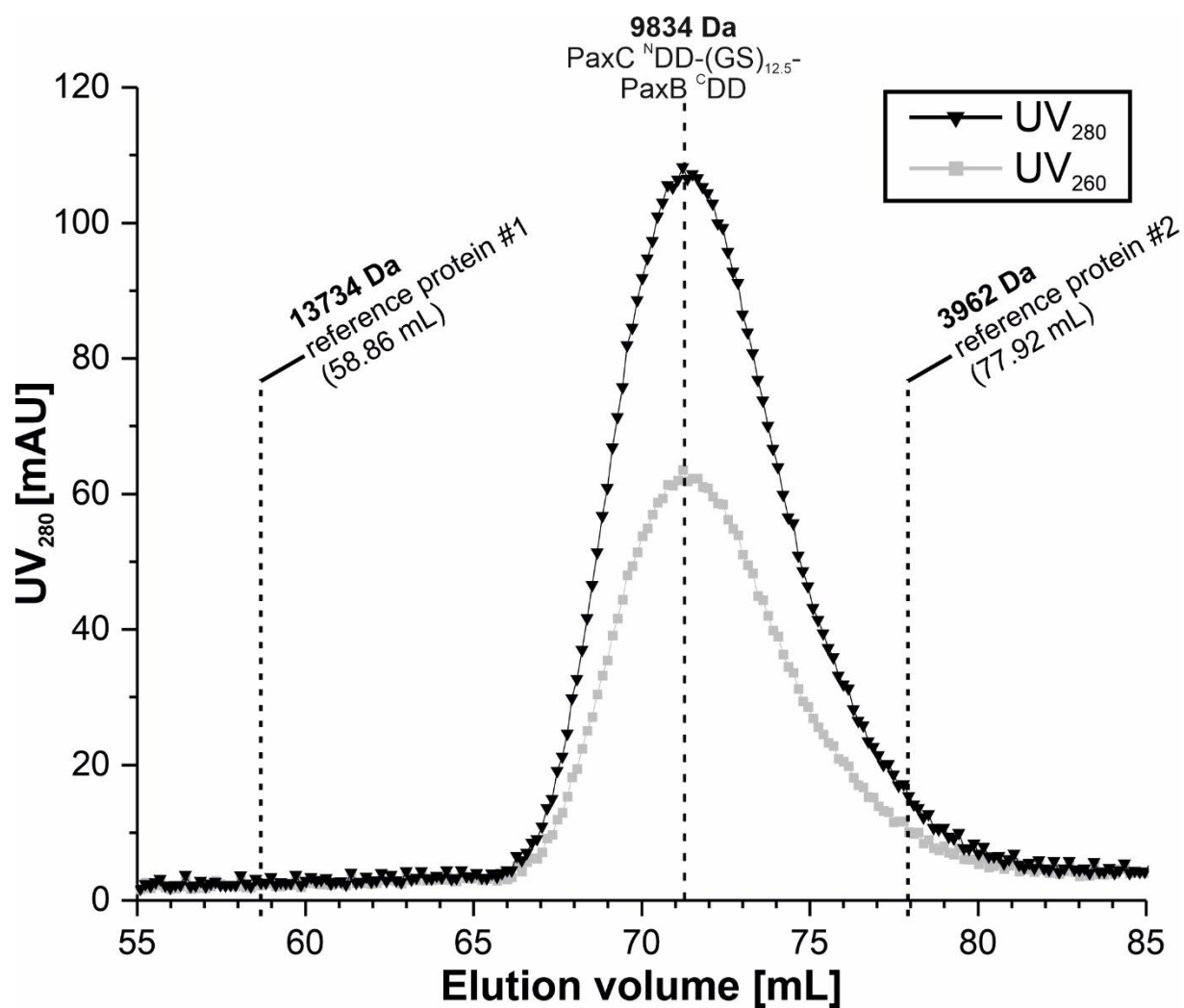
Figure S7. Chromatogram of the size exclusion chromatography (SEC) of the PaxC ^{N}DD-(GS)$_{12.5}$-PaxB ^{C}DD complex. In dashed lines the elution volume of two reference proteins (#1 & #2) and the GS-linked DD complex with the corresponding molecular weights is indicated.
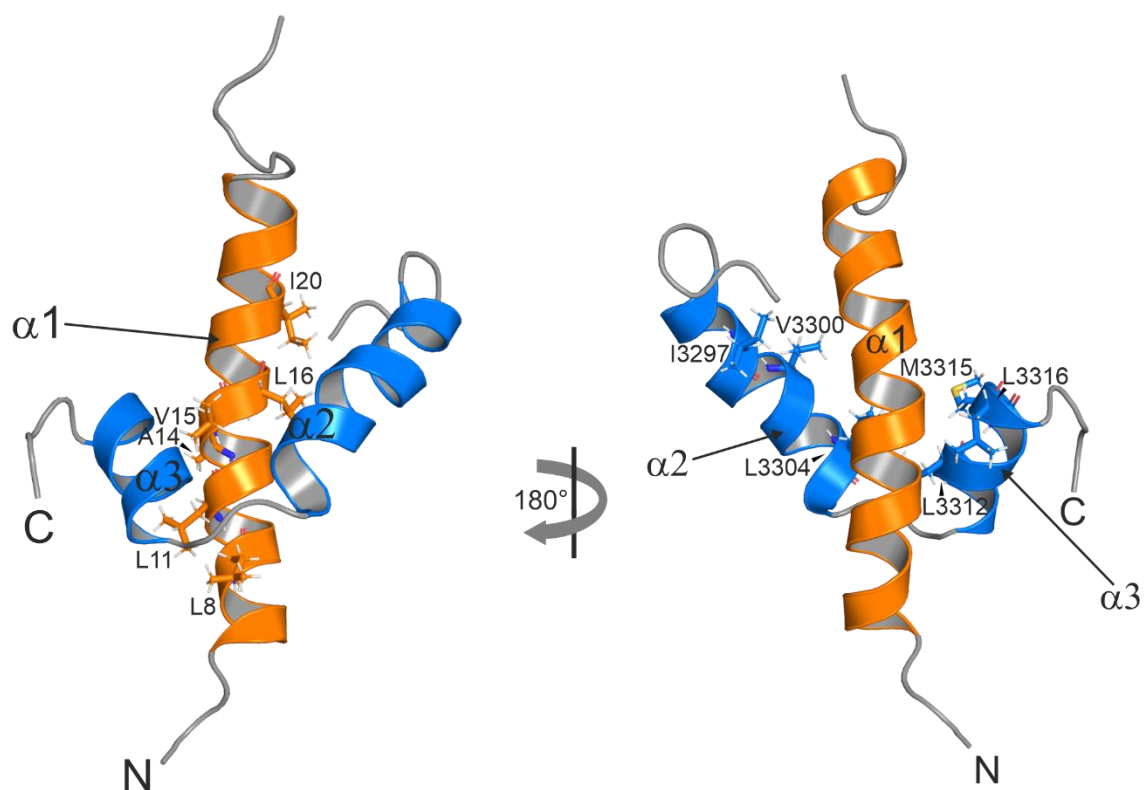
Figure S8. Hydrophobic interface of DD complex. Cartoon representation of the energy minimized structure of PaxC [N]DD (orange)-(GS)$_{12.5}$-PaxB [C]DD (blue) (linker is hidden) with the lowest target function. The hydrophobic residues which are involved in the DD interaction are highlighted as stick models.
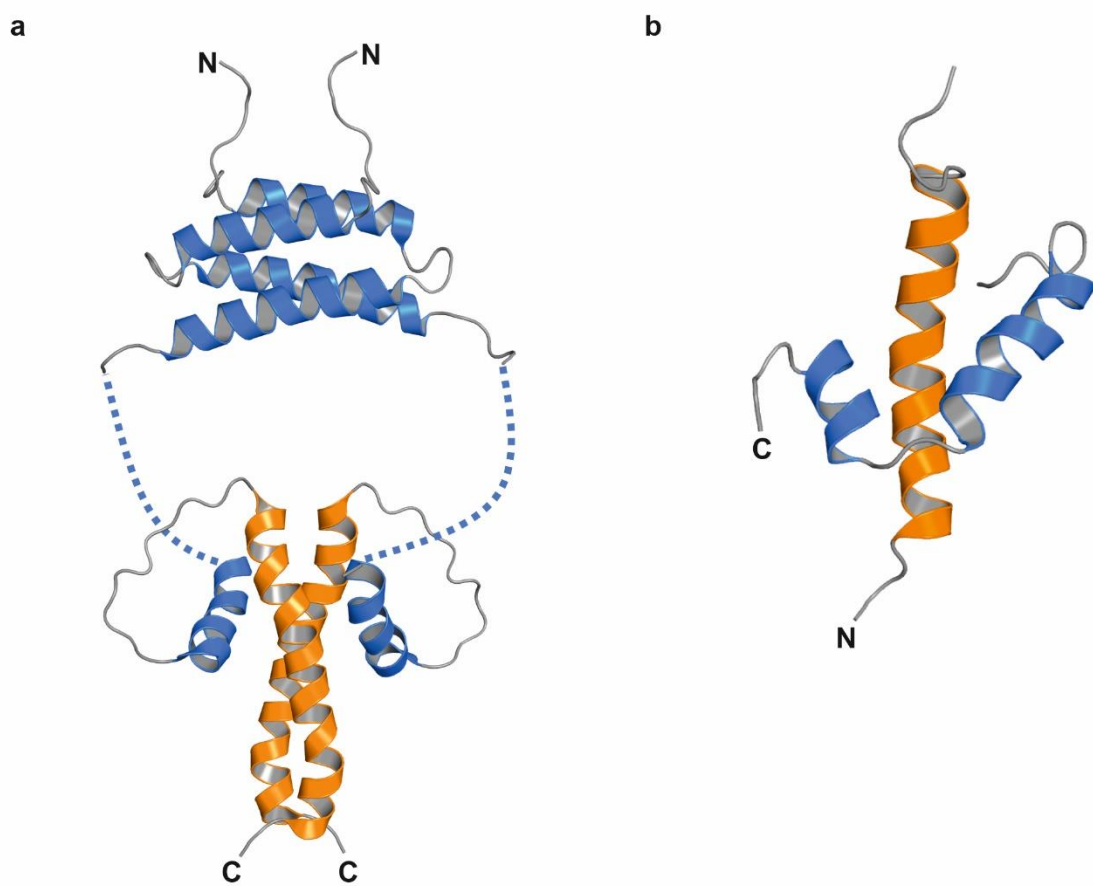
Figure S9. Docking Domain Class comparison. (a) NMR structure of a complex of covalently fused Class 1a docking domains (PDB: 1PZQ, 1PZR) (*8*) from a *cis*-AT PKS. The long, flexible linker connecting the second and third α-helices of the ^CDD is represented as a dashed line. (b) NMR structure of the newly identified Docking Domain type from the PAX peptide producing NRPS (GS-linker is hidden). C and N indicate C- and N-termini, respectively. The ^CDDs are coloured blue and the ^NDDs orange.

MATERIAL AND METHODS

General molecular biology

Molecular biology techniques like plasmid DNA preparation, transformation, restriction digestion and DNA gel electrophoresis, were adapted from standard protocols (*9*). Isolation of genomic DNA was carried out according to the manufacturer's instructions (QIAGEN). Q5High-Fidelity DNA-Polymerase (New England Biolabs) was used for PCR amplifications following the guide of the producer. PCR primers used in this study are listed in Table S3. All the plasmids (Table S2) generated in this study were constructed via Gibson assembly (*10*). The basic cloning was performed directly in the protein expression host *E. coli* BL21-Gold(DE3) (Agilent Technologies).

Expression and purification of DDs and DD complexes

For structure determination, $^{C/N}$DDs from *X. bovienii* (SS-2004) PaxB/C as well as the covalently linked ^{N}DD-^{C}DD complex and ^{N}DD mutants were heterologously expressed in *E. coli* BL21-Gold(DE3) under the control of a T7 promoter. The coding sequences were cloned into a modified pET11a vector containing an N-terminal His$_6$-SUMO tag, which allows cleaving off the tagged SUMO protein by ULP1 treatment. DNA fragments encoding PaxC ^{N}DD and PaxB ^{C}DD were linked with a 25 aa long GS linker in between. The resulting constructs were grown in uniformly ^{15}N and ^{15}N,^{13}C M9 minimal media containing 1 g L^{-1} ^{15}NH$_4$Cl (Cambridge Isotope Laboratories) or 1 g L^{-1} ^{15}NH$_4$Cl and 2.5 g L^{-1} ^{13}C$_6$-d-glucose (Cambridge Isotope Laboratories) and 100 mg mL^{-1} ampicillin. For ITC measurements, proteins were expressed in *E. coli* BL21-Gold (DE3) using LB medium. Protein expression was induced at an OD$_{600}$ of 0.6-0.8 with 1 mM IPTG overnight at 20 °C. After expression, cells were lysed by sonication in lysis buffer containing 50 mM Tris/HCl, pH 8.0, 300 mM NaCl, 10 mM MgCl$_2$, 1 mM EDTA, 0,5 µl pure Benzonase (Novagen), and

protease inhibitor (Roche). The lysate was cleared by centrifugation (30 min, 7500 × g, 4 °C) and the supernatant was passed through a Bio-Scale Mini Profinity Ni-charged IMAC Cartridge (Biorad) using HisTrap-buffer (50 mM sodium phosphate buffer (pH 8) with 150 mM NaCl and 500 mM imidazole for elution). The His$_6$-SUMO fusion tag was cleaved off by Ulp1 proteolytic digestion in dialysis buffer (50 mM Tris HCl, pH 8, 50 mM NaCl) and removed by a second purification step with the Ni-charged IMAC Cartridge using HisTrap-buffer. All three proteins (^{N}DD/^{C}DD and the ^{N}DD-^{C}DD complex) were further purified via SEC on a HiPrep 16/60 Sephacryl S-100 High Resolution column (GE Healthcare) in SEC buffer composed of 50 mM sodium phosphate buffer (pH 6.5) with 100 mM NaCl.

Construction of plasmids encoding modified DDs

DDs with amino acid exchanges were generated by site-directed mutagenesis using phosphorylated primers coding for the modified sequences. PCRs based on the wildtype DD expression plasmid were performed and the template was degraded by DpnI (Thermo Scientific) digestion. Finally, the PCR product with the specifically introduced mutation was ligated via T4 DNA ligase.

NMR spectroscopy

For NMR measurements, the DDs (0.5–1 mM) were prepared in 50 mM sodium phosphate buffer pH 6.5, 100 mM NaCl, and 10% D$_2$O. For NMR titration experiments, a protein concentration of 80 µM was used. NMR spectra were recorded at 20 °C on Bruker AVANCE III 600, 700, 800, and 950 MHz spectrometers equipped with cryogenic triple resonance probes. The proton chemical shifts were internally referenced to 2,2-dimethyl-2-silapentane-5-sulfonic acid and the heteronuclear ^{13}C and ^{15}N chemical shifts were indirectly referenced with the appropriate conversion factors (11). The standard set of triple resonance experiments

(HNCO, HN(CA)CO, HNCACB) was used for the backbone resonance assignments of the ^{C}DD of PaxB (*12*). For the PaxC ^{N}DD and the ^{N}DD-^{C}DD linker construct, BEST-TROSY versions of the triple resonance spectra were used (*13*). Shaped proton pulses with a bandwidth of 5.0 ppm centered at 8.5 ppm were used. The delay between scans was set to 0.3 s in all experiments. For side chain resonance assignment, 3D HBHA(CO)NH, (H)CCH-TOCSY, and H(C)CH-TOCSY experiments were used. All spectra were recorded and processed using Bruker TopSpinTM 3.5 and analyzed using the programs CARA (*14*) (www.nmr.ch) and CcpNmr Analysis (*15*). For titration experiments with NMR, the concentrations of the ^{C}DD peptide ((PaxB ^{C}DD, YQIETFFAQDIESVQKELENLSEEELLAMLNGDQQ (35 aa)); and ^{N}DD peptide ((PaxC ^{N}DD, MNINEQTLDKLRQAVLQKKIKERIQNSLSTEKY (33 aa)), were determined with UV-Vis spectroscopy. Therefore, a tyrosine was attached to the N-terminus of the ^{C}DD. For titration experiments, ^{1}H,^{15}N HSQCs or ^{1}H,^{15}N BEST-TROSY-HSQCs were recorded after the stepwise addition of lyophilized, unlabeled $^{C/N}$DD (25–480 µM) to a 80 µM ^{15}N-labeled $^{N/C}$DD protein sample. Before lyophylization the respective unlabeled peptide was rebuffered in ddH$_2$O. To evaluate NMR titration experiments, the chemical shifts were determined using the peak picking function of CcpNmr Analysis (*15*). The chemical shift differences were calculated using the following function (*16*).

$$(1)\ \Delta\delta = \sqrt{\Delta\delta_H^2 + \left(\frac{\Delta\delta_N}{6.5}\right)^2}$$

For the K_D determination based on the NMR titration experiments a quadratic saturation binding equation (*17*) was fitted to the concentration-dependent chemical shift changes of the relevant shifting peaks:

$$(2)\ \Delta\delta_{obs} = \Delta\delta_{max} \frac{[L_0] + [P_0] + K_D - \sqrt{([L_0] + [P_0] + K_D)^2 - 4[L_0][P_0]}}{2[P_0]}$$

Structure calculation

[15]N-nuclear Overhauser spectroscopy (NOESY)-HSQC, ^{13}C-NOESY-HSQC (aliphatic carbons), and ^{13}C-NOESY- HSQC (aromatic carbons) experiments in H_2O with mixing times of 250 ms were used to obtain distance restraints. The TALOS-N server was used to generate torsion angle restraints ([18]) based on backbone H, N, Cα, Cβ, and CO chemical shifts. Peak picking and NOE assignment was performed with the ATNOS/CANDID module in UNIO ([19]) in combination with CYANA ([20, 21]) using the 3D NOESY spectra. To correct falsely picked artefacts, the peak lists were reviewed manually and corrected. Distance restrains were obtained using the automated NOE assignment and structure calculation protocol available in CYANA (version 3.98) ([21]). An assignment of 87% of the observable NOESY crosspeaks for all NOESY spectra was achieved. Restrained energy refinement with OPALp ([22]) and the AMBER94 force field ([23]) of the 20 structures with the lowest target function was carried out. This set of CYANA generated, energy minimized structures with the lowest target functions were validated with the Protein Structure Validation Software (Table S4) suite1.5 ([5]). Electrostatic surface potential calculations were conducted with the PDB2PQR web server ([24]) using the PARSE force field and visualized with the APBS plug-in ([25]) for PyMOL with a threshold for electrostatic potential shading from -1 kT/e to +1 kT/e (k = Boltzmann's constant, T = absolute temperature, and e = electron charge (The PyMOL Molecular Graphics System, Version 2.1 Schrödinger, LLC). All figures of structures were prepared with PyMOL.

Isothermal Titration Calorimetry

ITC measurements were performed at 20 °C in 50 mM sodium phosphate buffer, pH 6.5, and 100 mM NaCl using a MicroCal iTC200 (Malvern Instruments) calorimeter. In all experiments, 50 µM of the respective docking partner [N/C]DDs were provided in the reference cell and the interaction partner, in a suitable concentration (PaxB [C]DD:

2000 µM, PaxC ^{N}DD R23E: 2100 µM, PaxC ^{N}DD K18A: 1380 µM), was added stepwise. ITC experiments started with an initial delay time of 120 s. The first injection of 0.2 µl was followed by 19 serial injections of 2 µl, separated by an interval of 180 s. For each experiment, the reference power was set to 11 µcal/s, stirring speed to 750 rpm and the high feedback mode was selected. Three independent titrations were performed for each DD pairs. The thermograms were processed using Origin7.0 (OriginLab) assuming a one site binding model. In all ITC measurements, a saturation of the binding partner, depicted by a clear plateau, was observed. This plateau was used for baseline correction. In titrations of PaxC ^{N}DD R23E the n-value had to been set to 1, fulfilling the expected one site binding, to have been able to calculate the K_D value.

Circular Dichroism

The circular dichroism spectra of PaxB/C $^{C/N}$DD and PaxC ^{N}DD-(GS)$_{12.5}$-PaxB ^{C}DD were recorded from 50 µM samples in 0.2-mm-path-length quartz cuvettes using a Jasco J-810 CD spectrometer equipped with a Jasco PTC-423S temperature control system. The buffer, 50 mM sodium phosphate buffer (pH 6.5) with 100 mM NaCl, was identical to that used to record NMR spectra. Data were collected at 0.5 nm increments from 260 to 195 nm at 293K.

HR-HPLC-ESI-MS

Purified DDs were analyzed via high resolution (HR)-HPLC-ESI-UV-MS using a Dionex Ultimate 3000 LC system (Thermo Fisher) coupled to an Impact II electrospray ionization mass spectrometer (Bruker) and a DAD-3000 RS UV-detector (Thermo Fisher). The protein samples were separated on a C3 column (Zorbax 300SB-C3 300Å, 150 mm x 3.0 mm x 3.5 µm, Agilent). ACN and H_2O w/ 0.1% (v/v) formic acid were used as mobile phases at a flow rate of 0.6 mL min^{-1}. HPLC was

performed with 30% ACN equilibration (0–1.5 min), followed by a gradient from 30-65% ACN (1.5–27 min) and a further elution step with 95% ACN (27–30 min). For internal mass calibration an ESI-L Mix (Agilent) was injected. The HPLC-MS analysis was set to positive mode with a mass range of m/z 50–2000 and an UV at 190–800 nm. For Data analysis of UV-MS-chromatograms Compass DataAnalysis 4.3 (Bruker) was used. The theoretical average masses of proteins were calculated using Compass IsotopePattern 3.0 (Bruker).

REFERENCES

1. Weiner, M. P.; Anderson, C.; Jerpseth, B.; Wells, S.; Johnson-Browne, B.; Vaillancourt, P. (**1994**) Studier pET system vectors and hosts. *Strateg. Mol. Biol. 7*.

2. Fuchs, S. W.; Proschak, A.; Jaskolla, T. W.; Karas, M.; Bode, H. B. (**2011**) Structure elucidation and biosynthesis of lysine-rich cyclic peptides in Xenorhabdus nematophila. *Org. Biomol. Chem. 9*, 3130–3132.

3. Chaston, J. M.; Suen, G.; Tucker, S. L.; Andersen, A. W.; Bhasin, A.; Bode, E.; Bode, H. B.; Brachmann, A. O.; Cowles, C. E.; Cowles, K. N.; Darby, C.; Léon, L. de; Drace, K.; Du, Z.; Givaudan, A.; Herbert Tran, E. E.; Jewell, K. A.; Knack, J. J.; Krasomil-Osterfeld, K. C.; Kukor, R.; Lanois, A.; Latreille, P.; Leimgruber, N. K.; Lipke, C. M.; Liu, R.; Lu, X.; Martens, E. C.; Marri, P. R.; Médigue, C.; Menard, M. L.; Miller, N. M.; Morales-Soto, N.; Norton, S.; Ogier, J.-C.; Orchard, S. S.; Park, D.; Park, Y.; Qurollo, B. A.; Sugar, D. R.; Richards, G. R.; Rouy, Z.; Slominski, B.; Slominski, K.; Snyder, H.; Tjaden, B. C.; van der Hoeven, R.; Welch, R. D.; Wheeler, C.; Xiang, B.; Barbazuk, B.; Gaudriault, S.; Goodner, B.; Slater, S. C.; Forst, S.; Goldman, B. S.; Goodrich-Blair, H. (**2011**) The entomopathogenic bacterial endosymbionts Xenorhabdus and Photorhabdus: convergent lifestyles from divergent genomes. *PloS one 6*, e27909.

4. Hacker, C.; Cai, X.; Kegler, C.; Zhao, L.; Weickhmann, A. K.; Wurm, J. P.; Bode, H. B.; Wöhnert, J. (**2018**) Structure-based redesign of docking domain interactions modulates the product spectrum of a rhabdopeptide-synthesizing NRPS. *Nat. Commun. 9*, 4366.

5. Bhattacharya, A.; Tejero, R.; Montelione, G. T. (**2007**) Evaluating protein structures determined by structural genomics consortia. *Proteins: Struct., Funct., Bioinf. 66*, 778–795.

6. Edgar, R. C. (**2004**) MUSCLE: a multiple sequence alignment method with reduced time and space complexity. *BMC bioinformatics 5*, 113.

7. Edgar, R. C. (**2004**) MUSCLE: multiple sequence alignment with high accuracy and high throughput. *Nucleic Acids Res.32*, 1792–1797.

8. Broadhurst, R.W.; Nietlispach, D.; Wheatcroft, M. P.; Leadlay, P. F.; Weissman, K. J. (**2003**) The Structure of Docking Domains in Modular Polyketide Synthases. *Chem. Biol. 10*, 723–731.

9. Sambrook, J.; Fritsch, E.; Maniatis, T. (**1989**) *Molecular cloning. A laboratory manual : Vol. 2*, 2. ed.; CSHL Press, New York.

10. Gibson, D. G.; Young, L.; Chuang, R.-Y.; Venter, J. C.; Hutchison, C. A.; Smith, H. O. (**2009**) Enzymatic assembly of DNA molecules up to several hundred kilobases. *Nat. Methods 6*, 343–345.

11. Markley, J. L.; Bax, A.; Arata, Y.; Hilbers, C. W.; Kaptein, R.; Sykes, B. D.; Wright, P. E.; Wüthrich, K. (**1998**) Recommendations for the presentation of NMR structures of proteins and nucleic acids--IUPAC-IUBMB-IUPAB Inter-Union Task Group on the standardization of data bases of protein and nucleic acid structures determined by NMR spectroscopy. *Eur. J. Biochem. 256*, 1–15.

12. Sattler, M. (**1999**) Heteronuclear multidimensional NMR experiments for the structure determination of proteins in solution employing pulsed field gradients. *Prog. Nucl. Magn. Reson. Spectrosc. 34*, 93–158.

13. Favier, A.; Brutscher, B. (**2011**) Recovering lost magnetization: polarization enhancement in biomolecular NMR. *J. Biomol. NMR 49*, 9–15.

14. Keller, R. L. J. (**2004**) The Computer Aided Resonance Assignment Tutorial [Online].

15. Vranken, W. F.; Boucher, W.; Stevens, T. J.; Fogh, R. H.; Pajon, A.; Llinas, M.; Ulrich, E. L.; Markley, J. L.; Ionides, J.; Laue, E. D. (**2005**) The CCPN data model for NMR spectroscopy: development of a software pipeline. *Proteins: Struct., Funct., Bioinf. 59*, 687–696.

16. Mulder, F. A.; Schipper, D.; Bott, R.; Boelens, R. (**1999**) Altered flexibility in the substrate-binding site of related native and engineered high-alkaline Bacillus subtilisins. *J. Mol. Biol. 292*, 111–123.

17. Williamson, M. P. (**2013**) Using chemical shift perturbation to characterise ligand binding. *Prog. Nucl. Magn. Reson. Spectrosc. 73*, 1–16.

18. Shen, Y.; Bax, A. (**2013**) Protein backbone and sidechain torsion angles predicted from NMR chemical shifts using artificial neural networks. *J. Biomol. NMR 56*, 227–241.

19. Herrmann, T.; Güntert, P.; Wüthrich, K. (**2002**) Protein NMR structure determination with automated NOE assignment using the new software CANDID and the torsion angle dynamics algorithm DYANA. *J. Mol. Biol. 319*, 209–227.

20. Güntert, P. (**2008**) Automated structure determination from NMR spectra. *Eur. Biophys. J. 38*, 129.

21. López-Méndez, B.; Güntert, P. (**2006**) Automated protein structure determination from NMR spectra. *J. Am. Chem. Soc. 128*, 13112–13122.

22. Koradi, R.; Billeter, M.; Güntert, P. (**2000**) Point-centered domain decomposition for parallel molecular dynamics simulation. *Comput. Phys. Commun. 124*, 139–147.

23. Ponder, J. W.; Case, D. A. (**2003**) Force fields for protein simulations. *Adv. Protein Chem. 66*, 27–85.

24. Dolinsky, T. J.; Nielsen, J. E.; McCammon, J. A.; Baker, N. A. (**2004**) PDB2PQR: an automated pipeline for the setup of Poisson–Boltzmann electrostatics calculations. *Nucleic Acids Res. 32*, 665-7.

25. Jurrus, E.; Engel, D.; Star, K.; Monson, K.; Brandi, J.; Felberg, L. E.; Brookes, D. H.; Wilson, L.; Chen, J.; Liles, K.; Chun, M.; Li, P.; Gohara, D. W.; Dolinsky, T.; Konecny, R.; Koes, D. R.; Nielsen, J. E.; Head-Gordon, T.; Geng, W.; Krasny, R.; Wei, G.-W.; Holst, M. J.; McCammon, J. A.; Baker, N. A. (**2017**) Improvements to the APBS biomolecular solvation software suite. *Protein Sci. 27*, 112–128.